The Near-Face Displacement of D-Shaped Tunnels in Isotropic & Anisotropic Media

Miguel A. Nunes

Graduate Student
Department of Civil Engineering and Applied Mechanics
McGill University, Montreal, Quebec, Canada
E-mail: miguel.nunes@mail.mcgill.ca

Mohamed A. Meguid

Assistant Professor
Department of Civil Engineering and Applied Mechanics
McGill University, Montreal, Quebec, Canada
E-mail: mohamed.meguid@mcgill.ca

ABSTRACT

Tunnels are crucial structures in the operation of many Civil Engineering works mainly because there are unique characteristics involved in designing and constructing them, namely the in-situ stresses due to overlaying rock or soil. Elastic theory has proven to be a useful aid in finding solutions and predicting accurately the displacements and stresses that arise from creating an opening within the ground. To this end, much work exists in the literature which addresses tunnel excavation by either investigating only the plane-strain deformations, or by studying the entire displacement profile of the tunnel periphery for the case where there is a uniform in-situ stress distribution in every direction. This paper seeks to conduct a broader investigation into the effects of elastic bi-directional in-situ stress distributions in both isotropic and anisotropic media in terms of radial closure along the entire length of the cavity, with specific attention given to the near-face region. The results presented are obtained from a parametric study based on full three-dimensional finite element analyses. The data are benchmarked using existing field data from the Darlington Intake Tunnel in Southern Ontario. The results of the study are then used for developing a simple expression and charts for predicting wall displacements along the entire length of a tunnel subjected to different in-situ stress conditions.

KEYWORDS: Deep tunnels, horizontal stresses, finite element, isotropic elasticity, convergence, anisotropic.

INTRODUCTION

Civil engineering projects such as hydroelectric works, transportation networks, and electricity power plants make use of tunnels for their operation. Tunnels are therefore crucial structures in the operation of these projects, and due care must be taken during the building phase in order for them to operate properly when the overall facility is in service. Unlike structures that are located at the surface, tunnels have the added challenges associated with subterranean conditions, or more specifically, those that arise from in-situ stresses due to overlaying soil or rock.

Consideration of these in-situ stresses is fundamental in the design and performance of many of the aforementioned structures. It is therefore of interest to the engineer to gain a comprehensive understanding of how these forces will affect the displacements around the opening, and how they are induced by excavating within different in-situ stress conditions. The first tool at an engineer's disposal is elasticity theory and how it can be applied to provide an initial estimation of circumferential displacements about a tunnel opening. Although the behaviour of soil or rock material is never truly elastic, the simplicity of all elastic solutions that predict stresses and displacements present an adequate preliminary insight into the effect of various parameters and variables. Elasticity theory is traditionally taught in terms of applying stresses to a medium that is initially unstressed. This is not true in the case of tunnelling applications, as openings are excavated out of rock or soil that are subject to in-situ stresses due to overburden pressures. Hence, the observed displacements around the periphery of the tunnel are the result of the release of these in-situ stresses. However soil and rock masses never exhibit truly elastic behaviour, but the simplicity of elastic methods that seek to predict stresses and displacements are especially useful tools in the cases of deep openings, where the effects and significance of various elastic parameters are of particular interest due to higher overburden pressures. To this end, much work exists in the literature that seeks to describe, model and predict these parameters, most notably of which are circumferential displacements. Treatments of these elastic problems can be found either in analytical form, or by numerical approximation.

Muir Wood (1975) developed analytical solutions for the case of a deep tunnel, and did so by seeking to correct the oversimplification of Morgan (1961), whose solution neglected shear stresses between extrados and ground (Muir Wood, 1975). Muir Wood's refinement took into account these interactions by inserting an explicit value for the interaction between the ground and lining in terms of shear stresses. He then extended his study by investigating the effects of changing one or more elastic parameter.

Pender (1980) approached the challenge of deriving elastic solutions for displacements analytically by analysing three idealised cases, each more realistic than the preceding one. First the problem was simplified to a square plate with a circularly drilled hole that was placed before stresses were applied to all four sides. The plate could either be of infinite or finite size. It was found that this case was applicable only in the instance where the stresses in the ground changed after excavation, such as heavy additional loading at the ground surface. The second approach was that of a tunnel excavated in a prestressed medium. The third and final case investigated the effects of the interaction between the ground and tunnel lining in a prestressed medium. Pender found that the displacements which occur when a circular opening is excavated in an elastic medium depend on the boundary conditions assumed in the derivation of the respective solutions.

Panet and Guenot (1982) used numerical modelling in their treatment. They idealised the problem by using a tunnel with a circular cross-section driven in a homogeneous, isotropic and elastic medium. They assumed that the initial stresses were isotropic as well. The solutions in the previous analytical approaches focused on the final theoretical displacements for the plane-strain region of a tunnel, or the displacements that would develop at many diameters away from the face of the advancing tunnel face. Panet and Guenot also had the advantage of using finite-element modelling to investigate the displacements of the

tunnel periphery in the region adjacent to the advancing tunnel face. Kumar (1987) aimed to study not only the effects of cross-anisotropy, but the effects of nonhomogeneity as well. This was done through the use of finite and infinite elements to simulate the near-field and far-field effects of both shallow and deep tunnel excavations.

Sharan (1989) used numerical approximations as well. The assumption of this work was that the tunnel was considered to be deep, so that the overlaying rock mass could extend to infinity in all directions. Sharan's work was based on a concept used in the modelling of unbounded fluid domains. It uses elastic supports around the finite-element model to simulate the effects of the unbounded rock. The expressions derived for the stiffness of these supports were found to depend on the shear modulus, Poisson's ratio of the rock medium, the ratio of horizontal to vertical initial stress, as well as the location of the elastic supports. Tonon and Amadei (2002) investigated the effect of elastic anisotropy on the convergence behind a tunnel face. They did this by means of a parametric study. Instead of using finite-element methods for their study, they utilized boundary-element modelling. Their work also matched closely with that of Corbetta et al. (1993) and Panet and Guenot (1982).

Carter and Booker (1990) used the work done by Sharpe (1942), Eringen (1957) and Selberg (1952), and extended it from the case of a merely spherically shaped opening to that of a long cylindrical cavity. Their solution is based in terms of Laplace transforms of the field quantities. Inversion of the transforms was performed numerically. Their work also focused on the significant differences between both the short and long term stress distributions as a result of rapid excavation. Corbetta et al. (1991) conducted a similar investigation with comparable assumptions, and also used finite-element methods for their modelling. The results of both works matched very closely and will be presented shortly hereafter.

Xiao & Carter (1993) utilised a boundary element formulation to evaluate the effect of jointing in anisotropic rock media. It was found that there was a good agreement between the numerical analyses and the available analytical analyses. Verruijt (1997) used a unique approach to deriving analytical solutions for the problem of excavation in an elastic medium, and did so through the use of complex variables. A half-plane was used in this model, whereby the upper boundary condition was free of stress. Laurent series expansions were used to represent the complex stress functions which were developed when the transformation from the real to the complex domain was done. This method had the advantage of being very general in character, thus enabling the solution of problems for various types of boundary conditions.

Singh et al. (1998) performed an investigation into the effect of the intermediate principal stress on the strength of an anisotropic rock mass. They concluded, among other considerations, that Mohr's theory should be modified for highly anisotropic material, especially jointed rock. This recommendation was made with an accompanying expression based on their findings which sought to account for the effect of the intermediate principal stress. Singh et al. (2004) performed an investigation into the effects of three-dimensional anisotropy by considering joints within a rock mass. By using readily available equations for elastic deformation, and by conducting a parametric study, they found that the tunnel closure in jointed rocks is highly anisotropic. Another conclusion was that the variation of any principal stress component affects the displacements around the opening significantly. Moreover the intermediate principal stress is as important in predicting displacements as are the major and minor stresses.

Much of the work published in the literature has addressed tunnel excavation by either investigating only the plane-strain deformations, or by studying the entire displacement profile of the tunnel periphery for the case where there is a uniform stress distribution in every direction. The objective of this paper is to present a study with particular interest of the displacement profile near the advancing face of a tunnel subjected to different lateral in-situ stress conditions for various elastic isotropic and anisotropic parameters. The proposed method provides a simple tool to predict the longitudinal displacement profile near the face of a deep tunnel under such conditions. It is based on full, three-dimensional finite-element analyses, and the developed expressions were formulated using a parametric study incorporating variable elastic properties, unit weights, and horizontal-to-vertical in-situ stress ratios. The results have been checked against field measurements taken at the Darlington Tunnel of Southern Ontario, which was excavated in limestone.

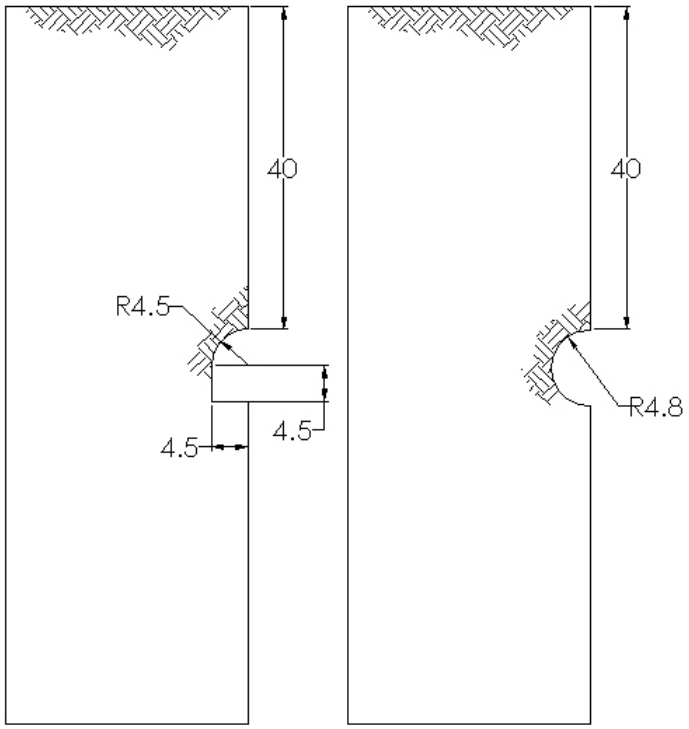

Figure 1. Elevation View of the Modelled Tunnel.

The tunnel section under consideration in this paper is a D-shaped tunnel situated in Southern Ontario (Figure 1). At the largest opening, the tunnel has a radius of 4.5 m, and measures 9 m from invert to crown. For the first treatment the rock mass is assumed to be both elastic and isotropic before, during and after the excavation. The second approach uses the assumption that the rock mass is both elastic and anisotropic before, during and after the excavation. The medium for both cases is also assumed to be homogeneous. The consideration of rock mass structure (rock joints, bedding planes, faults etc.) is beyond the scope of this study. The tunnel was modelled 40 m beneath the ground surface as measured from the springline, representing the case of a deep tunnel. Surface subsidence was therefore neglected. The excavation of the tunnel was simulated in 6 phases, each advancing the tunnel 10 m until a final length of 60 m from the opening to the tunnel face. There was also a further 60 m of medium that was modelled behind the face (Figure 2).

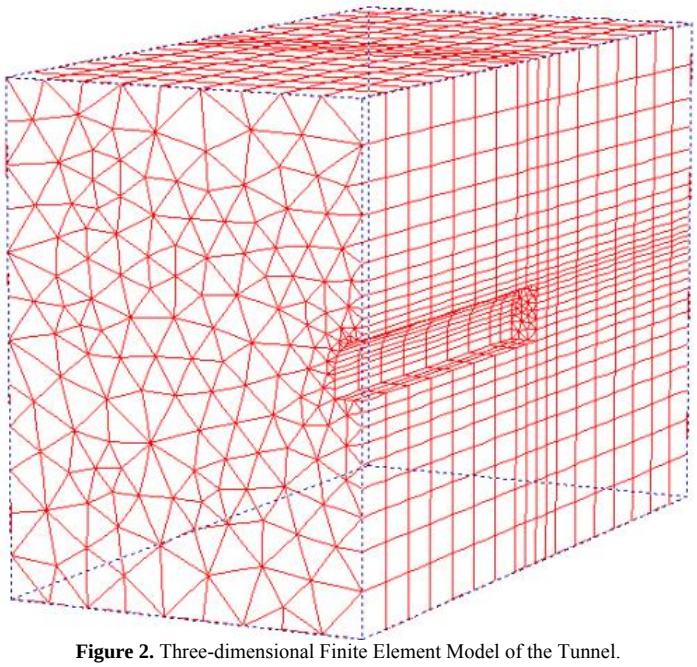

Figure 2. Three-dimensional Finite Element Model of the Tunnel.

NUMERICAL MODELLING

This paper is concerned primarily with the longitudinal displacements that occur after a tunnel as described above has been excavated, especially in the region immediately preceding the face advance, typically about four to five tunnel radii away from the face. The analyses were performed using the Plaxis 3D-Tunnel finite element program employing 15-noded wedge elements. The 3D finite element analysis was performed using 7020 fifteen-noded isoparametric wedge elements with a total of 19991 nodes arranged as shown in Figure 1. Nodes along the vertical boundaries of the mesh may translate freely along the boundaries but are fixed against displacements normal to these boundaries. The nodes at the base are fixed against displacements in both directions. The stage of excavation which is depicted in the figure is the final phase. Furthermore the software was enabled only to model elastic isotropic and anisotropic behaviour.

Methodology

Three variables, E, ν and γ, were used in the parametric study for the isotropic case. Two were held constant while the other was allowed to change. E varied from 20 to 30 GPa, ν from 0.27 to 0.33, γ from 20 to 25 kN/m^3, and each set of cases was analysed for K_0= 1, 2, 4, 6, 8, 10. To check the numerical results of this analysis against existing solutions, the cases for K_0 = 1 were plotted along with the solutions provided by Panet and Guenot (1982) and by Corbetta et al. (1991). A typical example of the tunnel convergence is shown in Figure 3, and it can be seen that the calculated displacements matched quite favourably with the predicted values of the solutions mentioned above. The plane-strain data at the springline and crown in the numerical model were also compared with the analytical solutions provided by Hefny & Lo (1999). The values at the crown matched quite well, whereas the values at the springline were always within at least 86% of the predicted value. This difference can be explained by the fact that the analytical solution was based on an ideal circular opening in an elastic medium, while the numerical model that was used was based on a D-shaped tunnel. Each set of data was trimmed to show only the displacements beginning at the face of the tunnel wall, and ending where apparent plane-strain conditions existed. Displacements were then plotted versus distance from the tunnel face. Regression was performed, and equations were produced for the crown and for the springline.

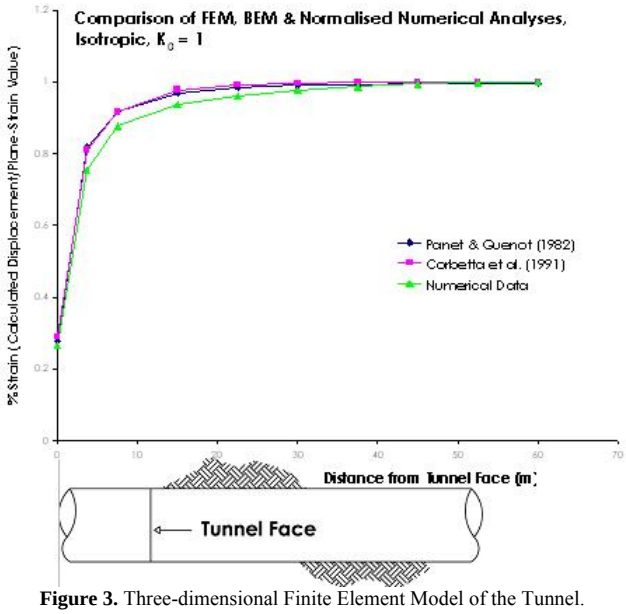

Figure 3. Three-dimensional Finite Element Model of the Tunnel.

The parametric study for the anisotropic case was done in a similar fashion to the isotropic case where the following elastic parameters were varied (ranges are presented in square parentheses):

Poisson's ratio in the horizontal direction (ν_h) [0.20 to 0.40], the Poisson's ratio for strain in the vertical direction due to horizontal stress (ν_{vh}) [0.20 to 0.40], and the effect of the ratio between the Young's modulus in the horizontal direction and the shear modulus in the vertical direction due to stress in the horizontal direction (E_h/G_{vh}) [3.0, 6.0 and 10].

All of these parameters were altered as the ratio between horizontal and vertical stresses was held constant at K_0 = 1, 5, 10. The unit weight of the medium was also held constant at 25 kN/m^3 for all cases.

RESULTS

Certain trends were noticed after examining all of the data. They can be seen in the following figures, and will be described as they are presented. By first using the Darlington site conditions to benchmark the results, each elastic variable was chosen individually and changed appropriately for a range of values. This facilitated a detailed investigation into the effect that one variable would have on the plane strain displacements at the crown and springline. All displacement data were normalised according to the following relation,

$$\Omega = \frac{uE}{aP_0}$$

where negative values correspond with inward movement.

Isotropic Analyses

Effect of E

As shown in Figures 4 and 5 (a through c) a higher modulus value led to smaller displacements. At 20 GPa the displacement at the crown was estimated at 0.62 mm, and at 4.3 mm at the springline, while at 30 GPa, the values were 0.41 mm and 2.9 mm respectively. This was a direct consequence of the strength of the medium increasing. Also noticed were that the calculated displacements were more or less constant for the K_0 = 1, 2 cases for both the crown and springline.

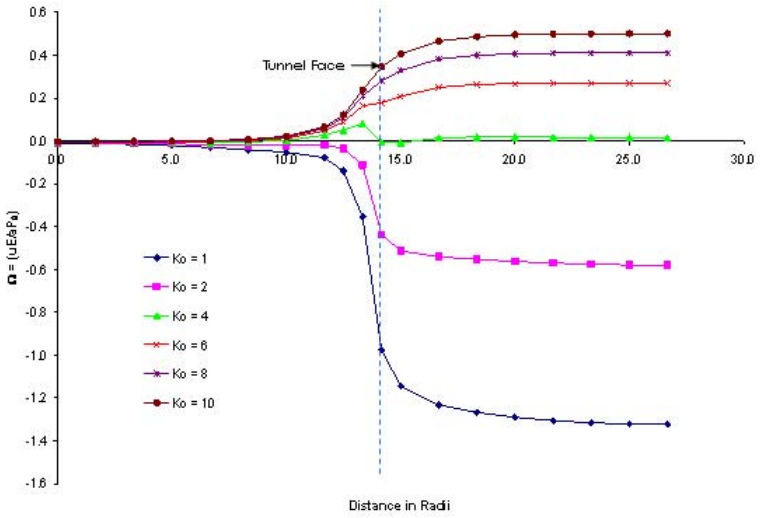

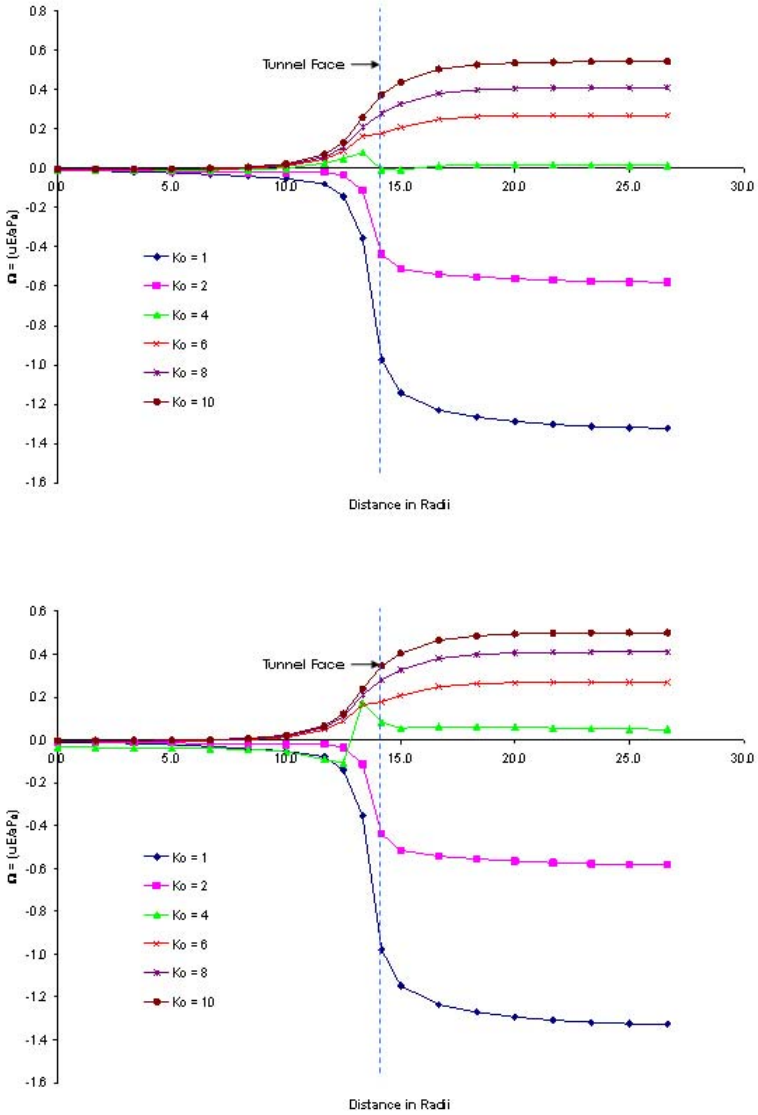

Figure 4. Effect of Changing E at the Crown; (a) E = 20 GPa, (b) E = 25 GPa, (c) E = 30 GPa.

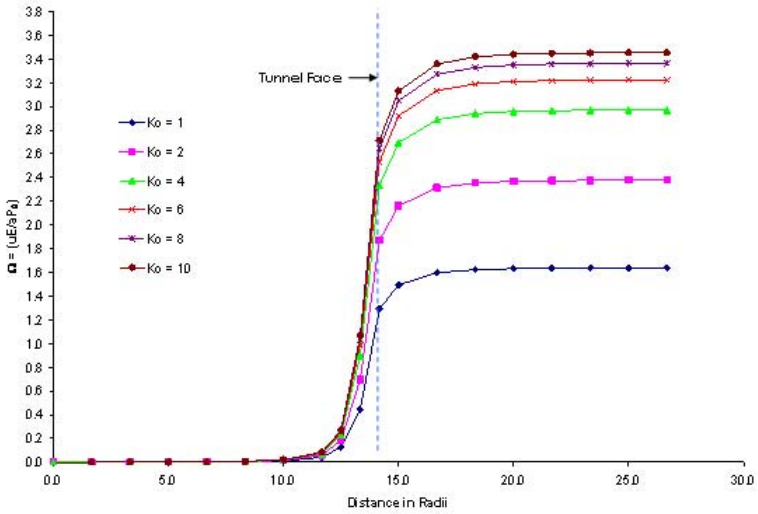

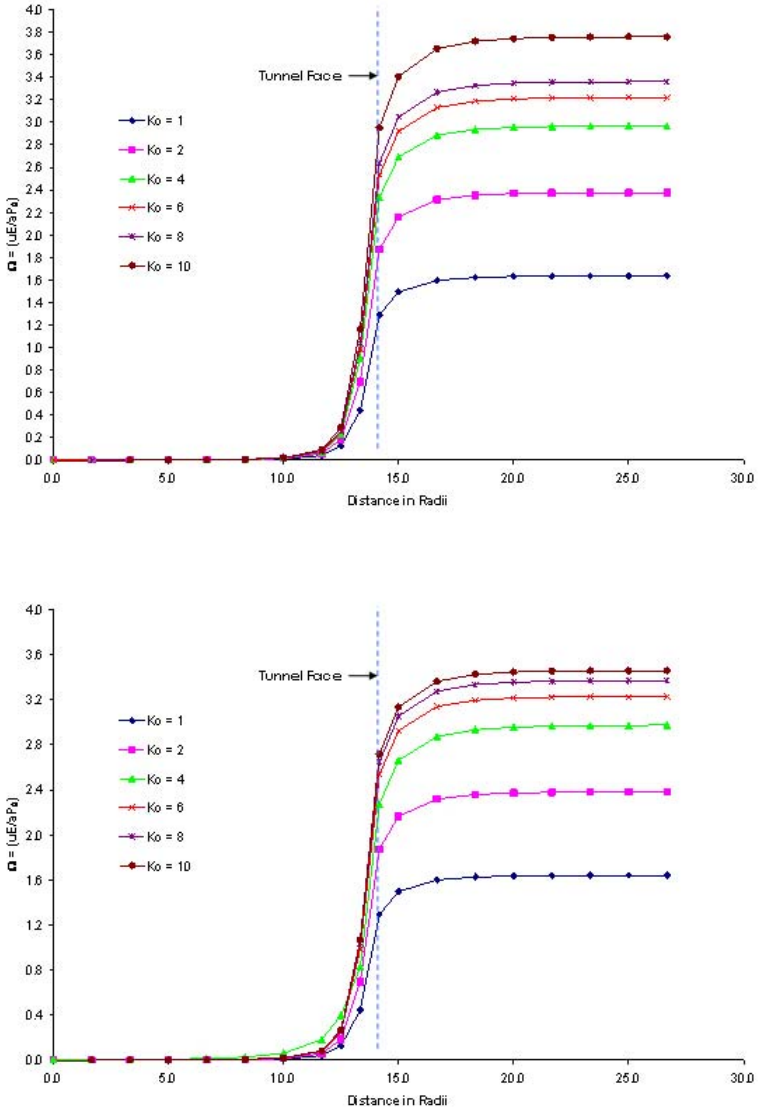

Figure 5. Effect of Changing E at the Springline; (a) E = 20 GPa, (b) E = 25 GPa, (c) E = 30 GPa.

Changing ν also had a significant effect (Figures 6 and 7), as a value of ν = 0.30 had displacements of 0.59 mm and 3.2 mm for crown and springline, respectively. When the value was changed to ν = 0.27, the displacements were 0.64 mm and 2.90 mm, respectively.

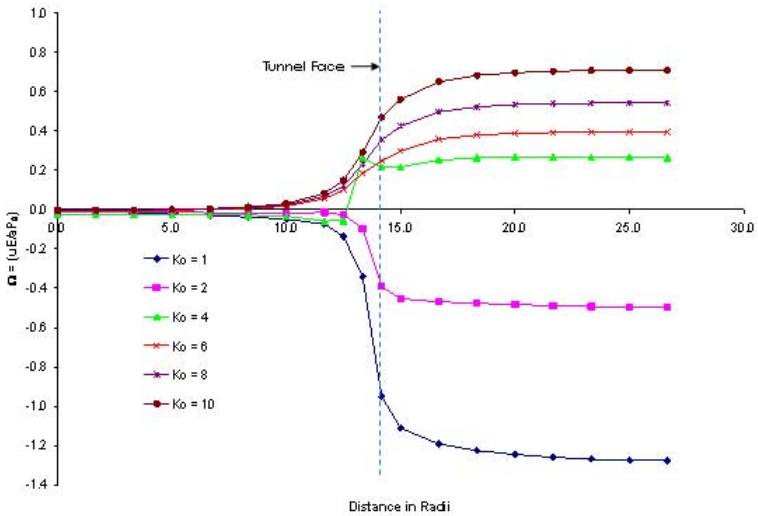

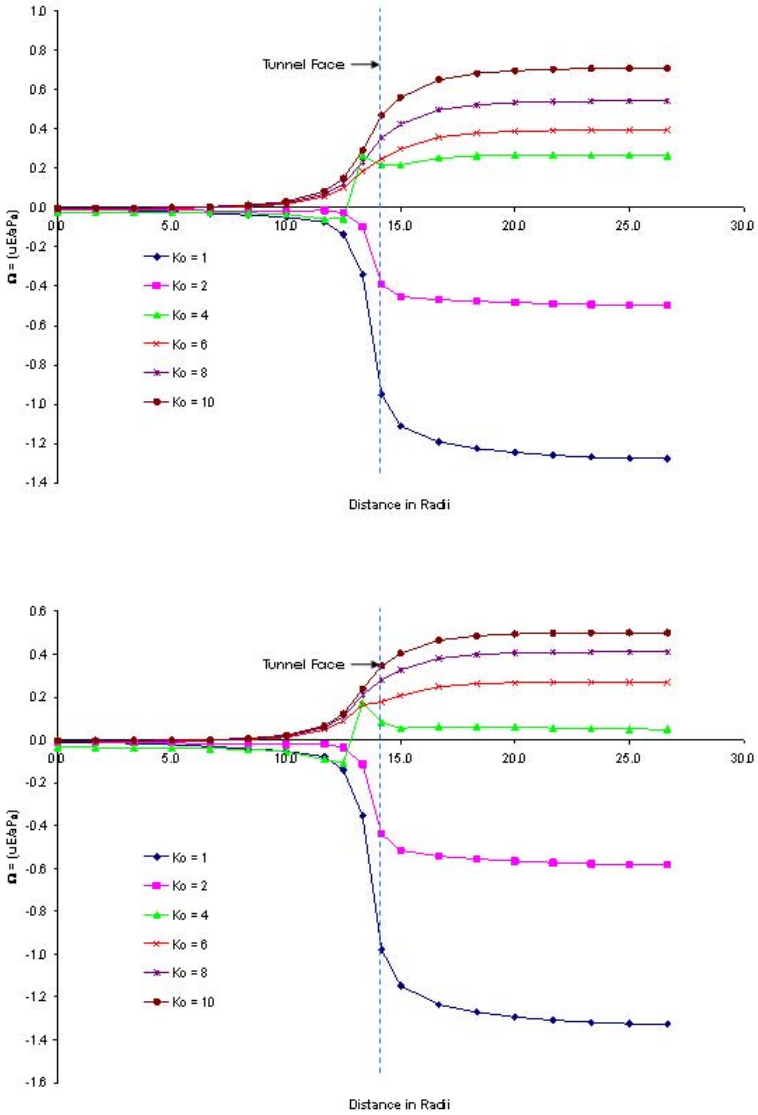

Figure 6. Effect of Changing ν at the Crown; (a) ν = 0.27, (b) ν = 0.30, (c) ν = 0.33.

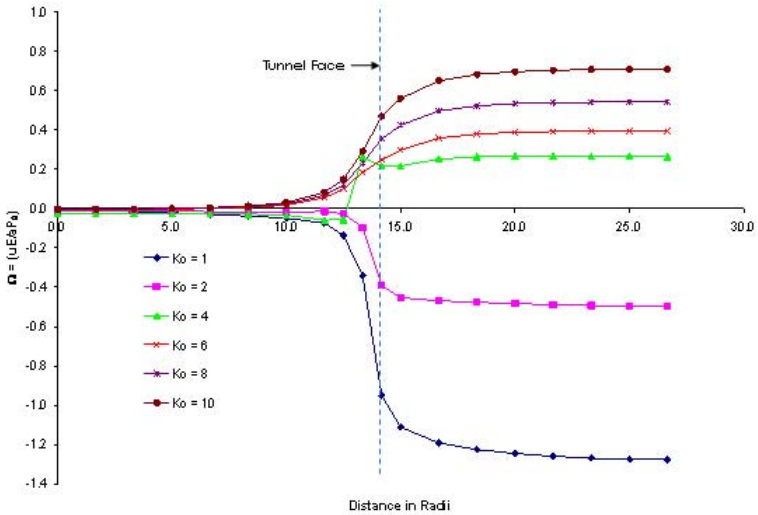

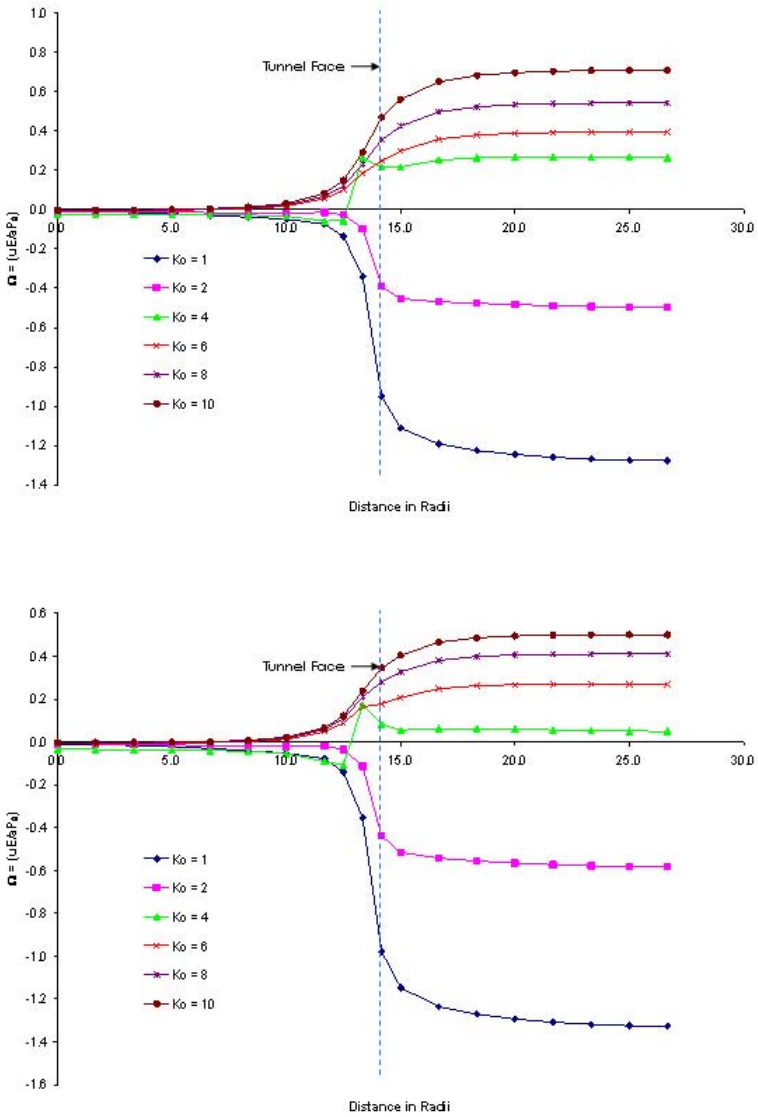

Figure 7. Effect of Changing ν at the Springline; (a) ν = 0.27, (b) ν = 0.30, (c) ν = 0.33.

Effect of Changing γ

The variation of the unit weight had the least effect on the displacements (Figures 8 and 9). For $\gamma = 20$ kN/m^3, the displacements were 0.33 mm and 2.3 mm, and for $\gamma = 22.5$ kN/m^3 they were 0.37 mm and 2.6 mm. The elastic parameters were all varied one at a time in similar fashion to the examples presented above, while the others were held constant. However the aforementioned trends were seen to repeat. Furthermore, the displacements at or near the face of the tunnel followed similar patterns as illustrated by the plane strain values. For these reasons, the unit weight was held constant for all of the anisotropic cases.

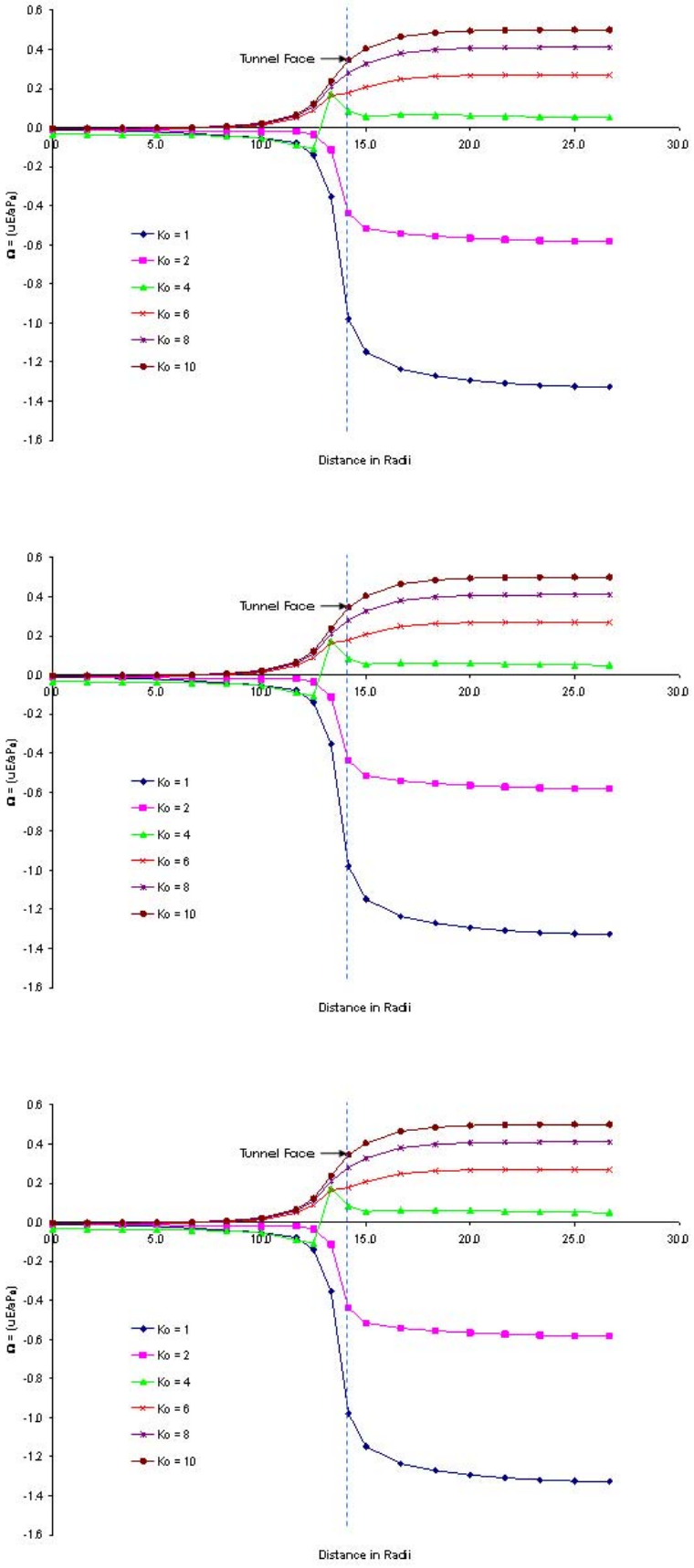

Figure 8. Effect of Changing γ at the Crown; (a) γ = 20 kN/m^3, (b) γ = 22.5 kN/m^3, (c) γ = 25 kN/m^3.

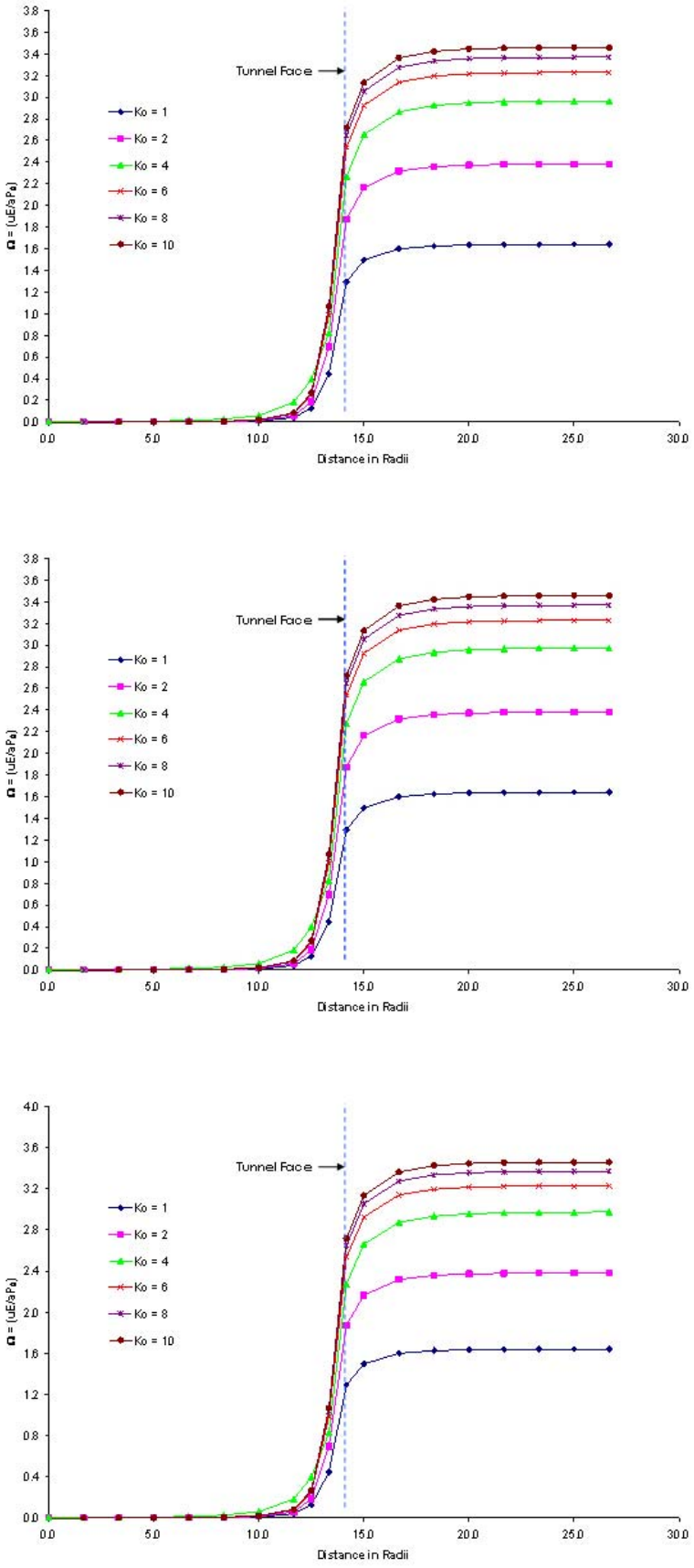

Figure 9. Effect of Changing γ at the Springline; (a) γ = 20 kN/m^3, (b) γ = 22.5 kN/m^3, (c) γ = 25 kN/m^3.

Anisotropic Analyses

Effect of ν

Varying ν_h between 0.20 and 0.40 had an appreciable and mostly uniform effect on the displacements at the crown and springline when $K_0 = 1$ (Figures 10 and 11). All of the movement at the crown was inward and ranged from plane-strain values of 0.18 mm at $\nu_h = 0.20$ to 0.22 mm at $\nu_h = 0.40$. The calculated displacements at the springline were as expected but slightly higher than the values at the crown at 0.28 mm and 0.32 mm, respectively. As K_0 was changed to 5 the displacement pattern was not as uniform as the case of $K_0 = 1$. First, all of the movement at the crown was upward. Second, the spread of the values for the displacements was much greater, beginning at 0.39 mm ($\nu_h = 0.20$) and 0.12 mm ($\nu_h = 0.40$). Finally, the pattern of displacement was not fully uniform. There was a deviation in the case of $\nu_h = 0.40$, where calculated displacements were approximately constant from the face of the tunnel to edge of the opening. The pattern was different at the springline; the displacements for all values of ν_h were virtually the same, ending at a plane strain value of about 1.80 mm. A regular pattern of displacement appeared at the crown when K_0 was changed to 10, and varied between 1.10 mm and 0.54 mm. As in the case where $K_0 = 5$, the displacements for all values of ν_h seemed to converge, ending at a plane-strain value of about 3.60 mm.

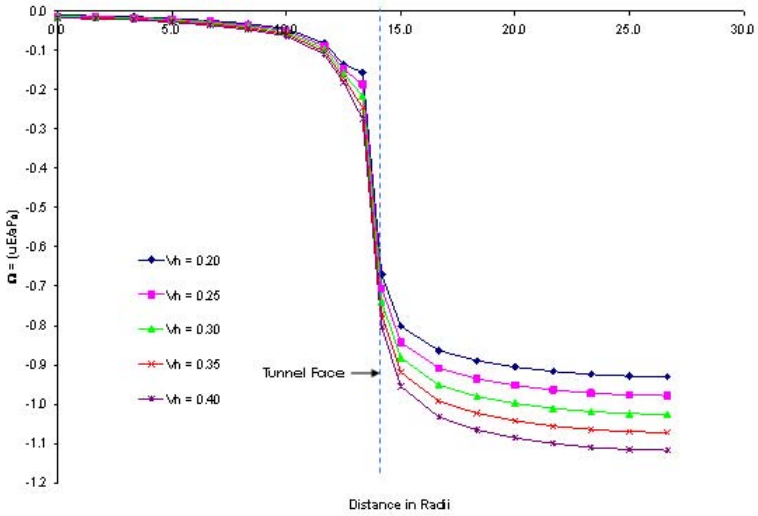

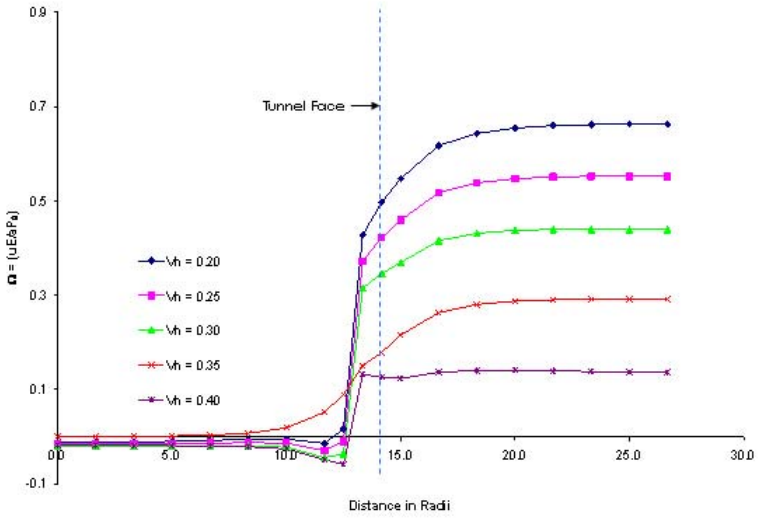

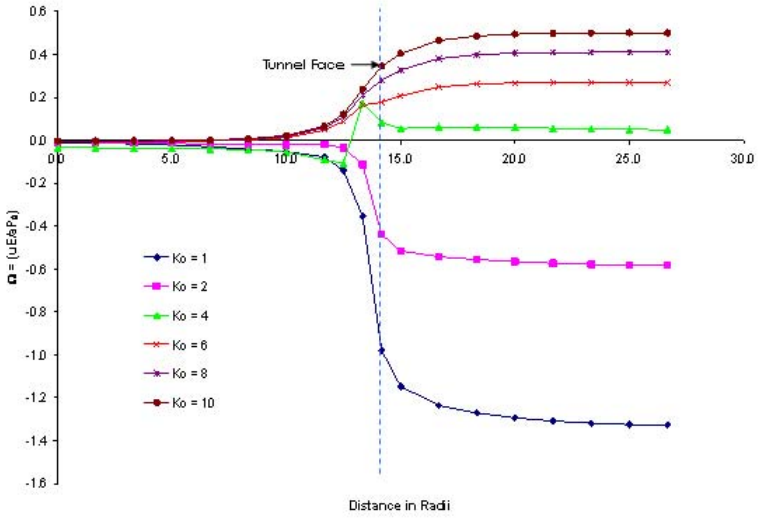

Figure 10. Effect of Changing ν_h at the Crown; (a) $K_0 = 1$, (b) $K_0 = 5$, (c) $K_0 = 10$.

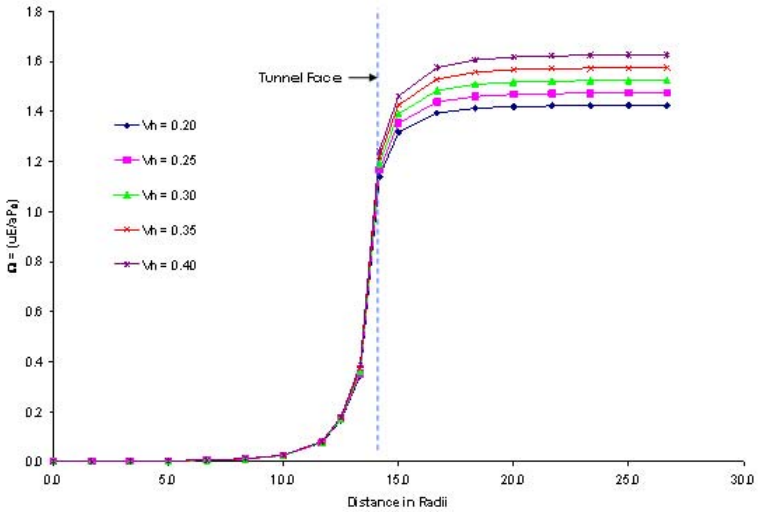

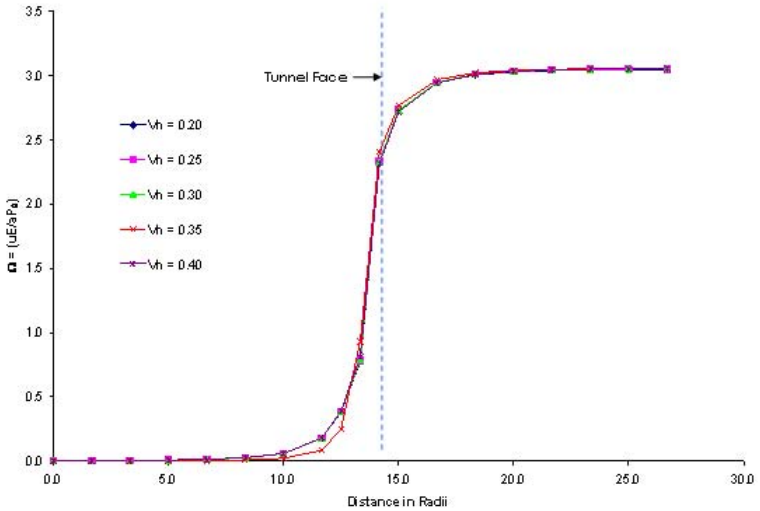

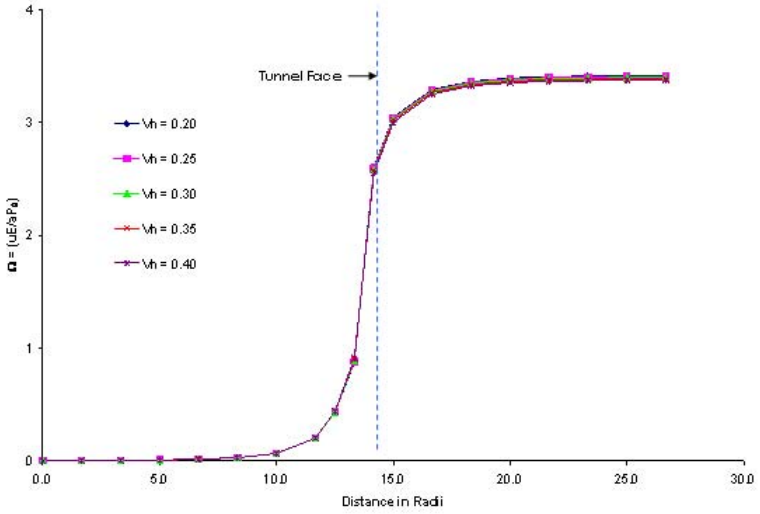

Figure 11. Effect of Changing ν_h at the Springline; (a) $K_0 = 1$, (b) $K_0 = 5$, (c) $K_0 = 10$.

When $K_0 = 1$, the pattern of displacements was the same for the same case ν_h, where all of the movement was inward (Figures 12 and 13). However the spread of the values was not as large, with a plane-strain displacement of 0.24 mm ($\nu_h = 0.20$) and 0.26 mm ($\nu_{vh} = 0.40$). The pattern at the springline was similar: 0.35 mm and 0.33 respectively. The case where $K_0 = 5$ once again displayed an interesting deviance from the regular pattern that developed for $K_0 = 1$. The movement at the crown was generally upward, but as ν_h increased (especially for $\nu_{vh} = 0.35, 0.40$), the displacements decreased in the vicinity immediately adjacent to the face of the tunnel ($0 < d < 7.5$ m) and then began significantly increasing after this point. The range of displacements were 0.33 mm ($\nu_{vh} = 0.20$) and 0.23 mm ($\nu_{vh} = 0.40$). The values at the springline showed regularity but with very little spread: 2.12 mm and 1.95 mm respectively. Once again a regular patter was seen at the crown when K_0 was changed to 10, with increasing values of displacement which is rapid near the face and approaches plane-strain near the opening. The displacements ranged from 1.04 mm to 0.84 mm. A similar trend was observed at the springline with a range from 4.34 mm to 3.98 mm.

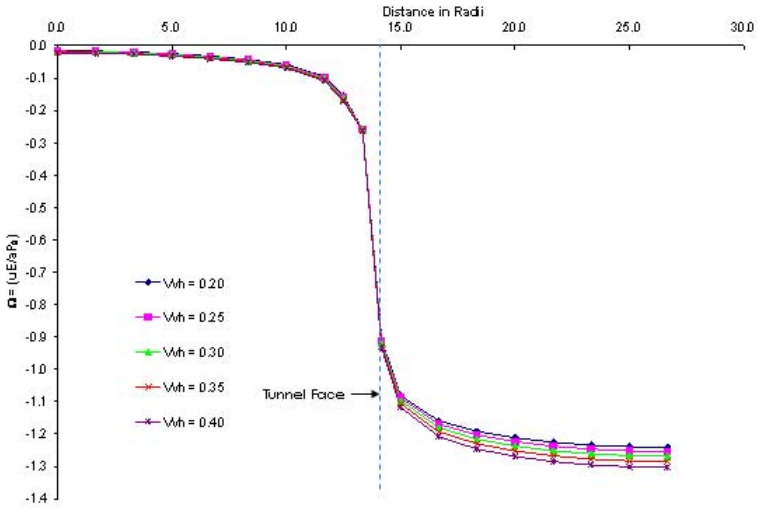

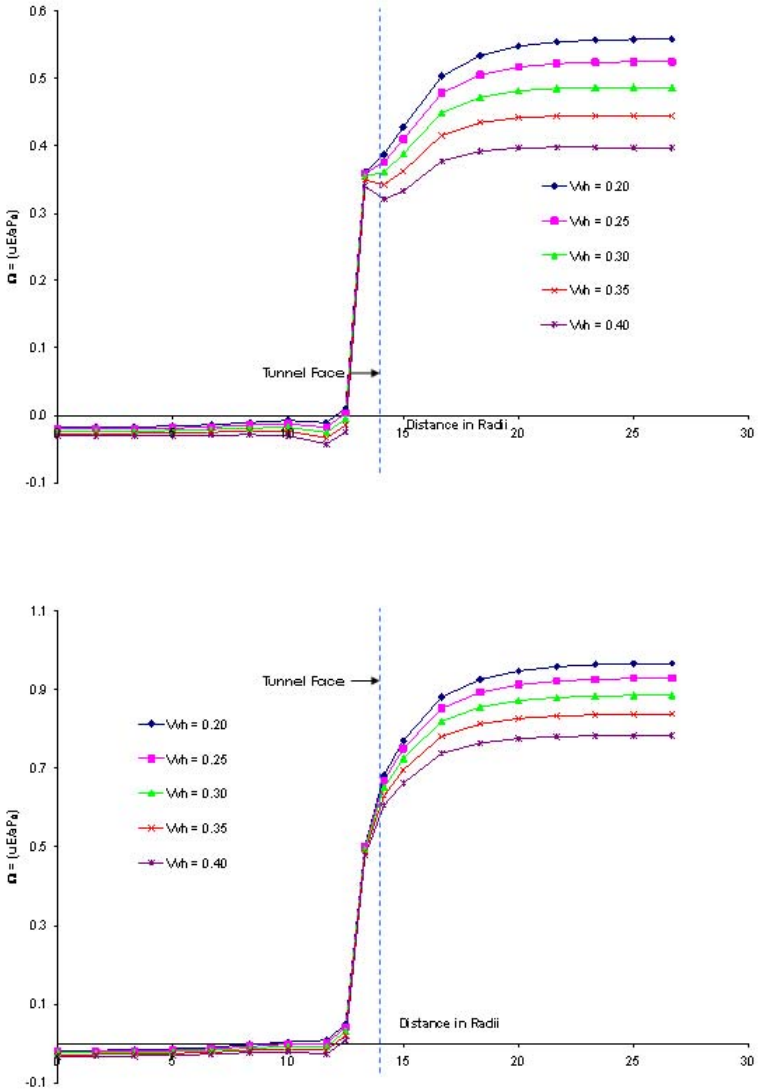

Figure 12. Effect of Changing ν_h at the Crown; (a) $K_0 = 1$, (b) $K_0 = 5$, (c) $K_0 = 10$.

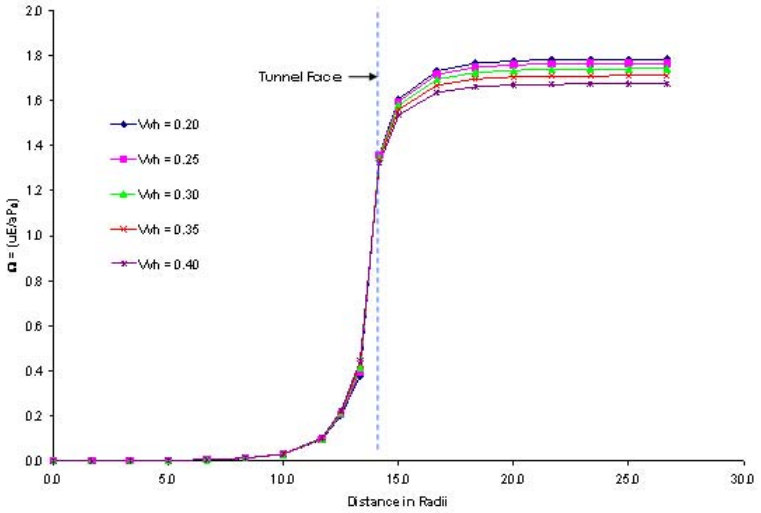

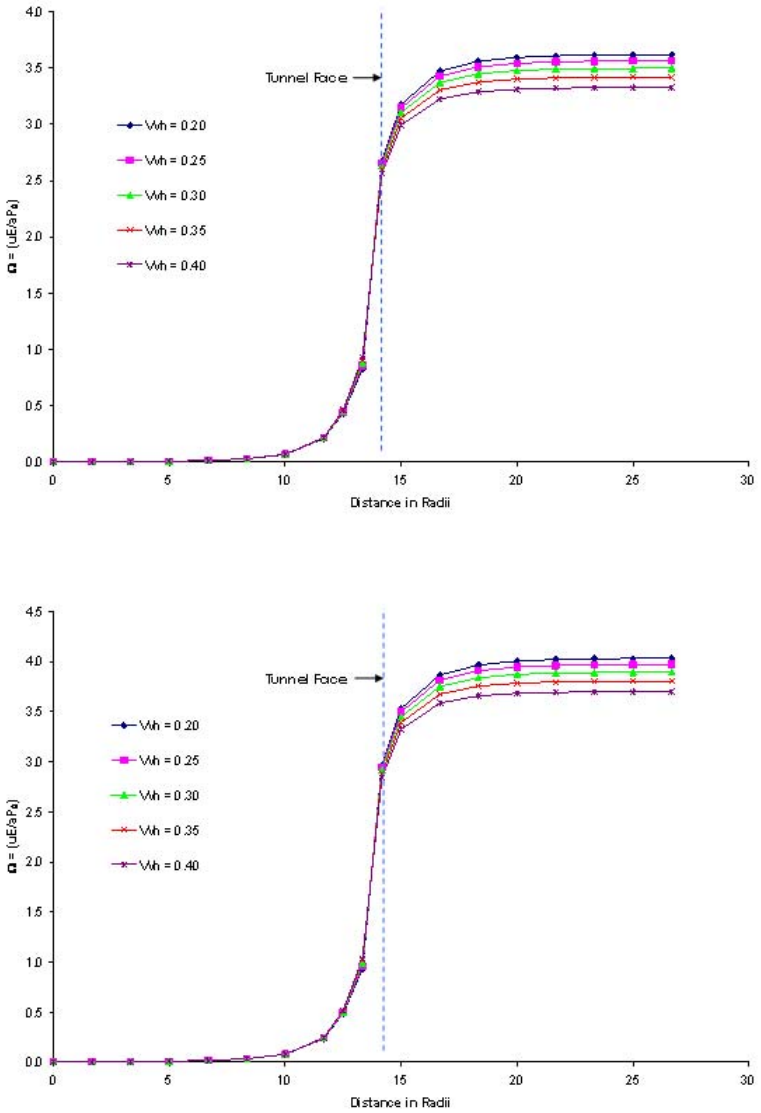

Figure 13. Effect of Changing ν_h at the Springline; (a) $K_0 = 1$, (b) $K_0 = 5$, (c) $K_0 = 10$.

Effect of E_h/G_{vh}

The case when $K_0 = 1$ resulted in similar patterns as presented above (Figures 14 and 15). However the spread in values was much greater; there was an inward movement of 0.21 mm for $E_h/G_{vh} = 3.0$, 0.32 mm for $E_h/G_{vh} = 6.0$, and 0.45 mm for $E_h/G_{vh} = 10$. The previously noticed trend was also the same at the springline and yielded the following values: 0.31 mm, 0.42 mm and 0.53 mm, respectively. The trend in displacement pattern followed the case where ν_{vh} was changed once $K_0 = 5$. The displacements for $E_h/G_{vh} = 6$, 10 decreased in the zone close to the face and began to resume the usual pattern of gradual increase at $d = 7.5$ m. The plane-strain values were 0.34 mm, 0.23 mm and 0.10 mm. The trend at the springline was one of increasing displacement that gradually converges at a plane-strain value. The values were 1.91 mm, 2.45 mm and 2.99 mm, respectively. The expected trend was seen when $K_0 = 10$ with upward plane-strain movements of 1.03 mm, 0.92 mm and 0.78 mm, while at the springline the values were 3.91 mm, 4.98 mm and 6.06 mm, all respectively.

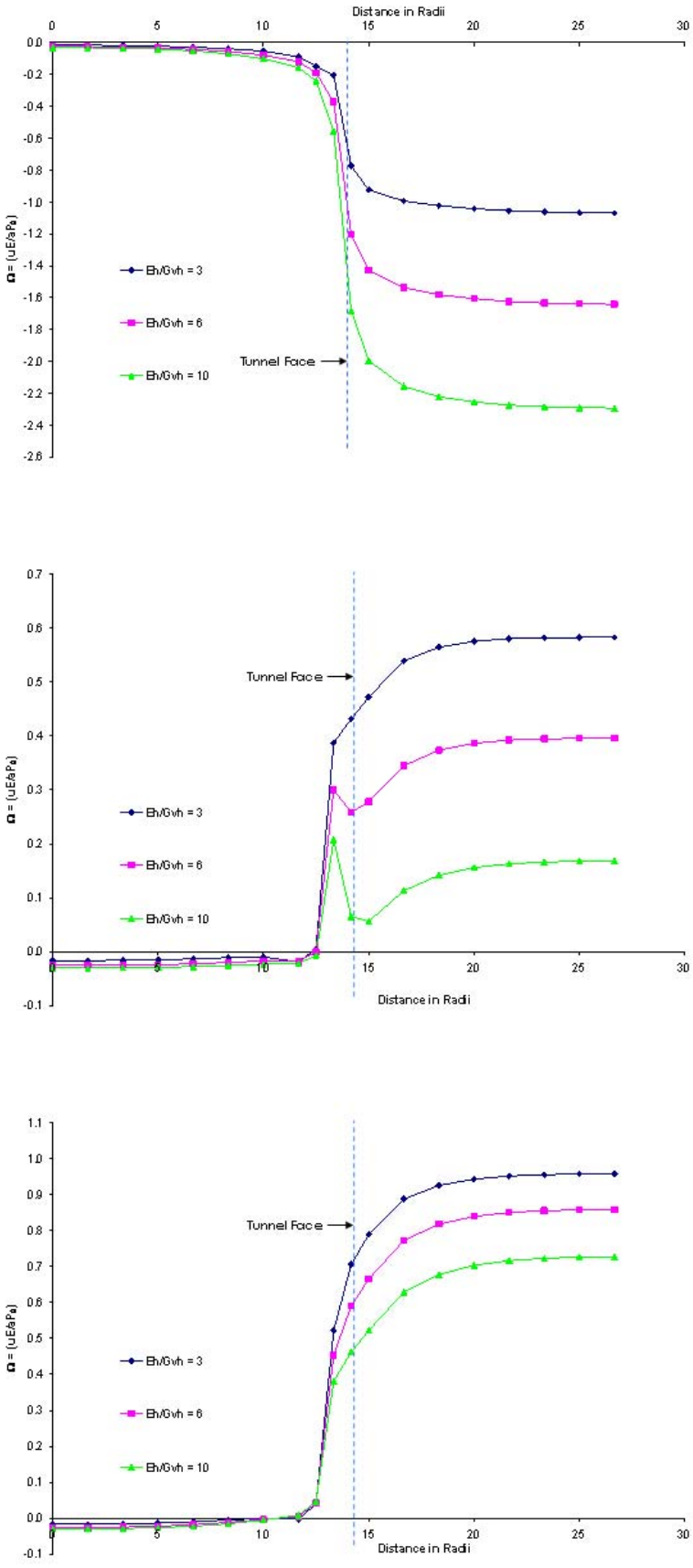

Figure 14. Effect of E_h/ G_{vh} at the Crown; (a) $K_0 = 1$, (b) $K_0 = 5$, (c) $K_0 = 10$.

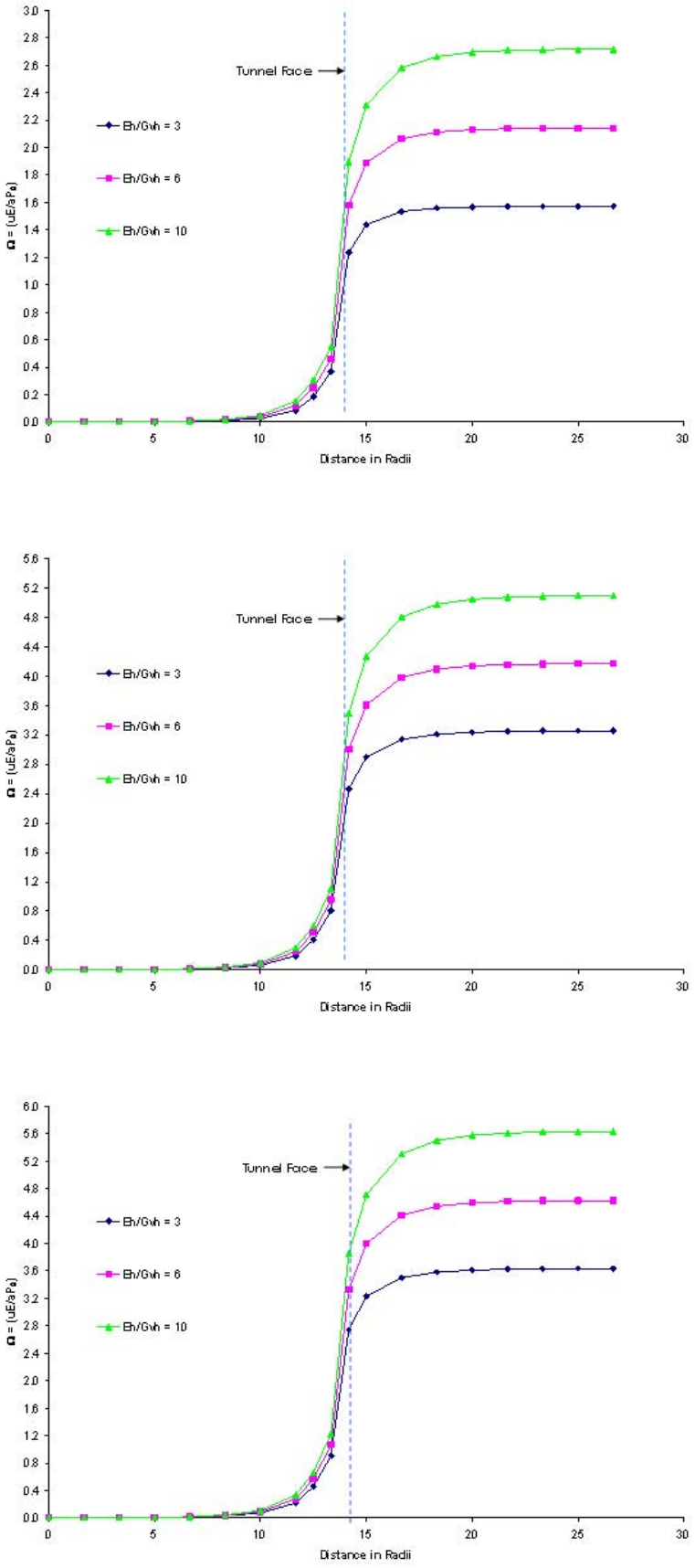

Figure 15. Effect of E_h/ G_{vh} at the Springline; (a) $E_h/ G_{vh} = 3$, (b) $E_h/ G_{vh} = 6$, (c) $E_h/G_{vh} = 10$.

Predicting Displacements

The Darlington case allowed for significant benchmarking of the data. Insodoing it also facilitated the generation of two parametric equations that were used

to estimate the displacements at the crown and springline for any given E, γ, ν, or K_0. The equations are empirical and take the forms as follows.

$$u_c = \frac{0.259 m_1 R P_0}{E}\left[1.926 m_2 - \exp\left(\frac{-0.605 m_3 d}{R}\right)\right] \quad (1)$$

$$u_s = \frac{2.363 n_1 R P_0}{E}\left[1.455 n_2 - \exp\left(\frac{-1.354 n_3 d}{R}\right)\right] \quad (2)$$

where m_1, m_2, m_3 and n_1, n_2, n_3 are constants that are dependent on E, γ, ν, and K_0. These constants can be determined using the charts found in the appendix. The equations were created by performing regression on normalised displacement values for each trial. The data were truncated where the face of the tunnel was modelled and extended until the simulated tunnel opening. Therefore these equations are valid from the face of the tunnel ($d = 0$) until a relatively large distance away from the face ($d = \infty$). They only apply to the isotropic cases as the anisotropic scenarios have displayed significant differences in trends that do not lend well for the normalisation process.

Example: The Darlington Tunnel

The Darlington G.S. is a D-shaped nuclear electricity generating facility situated 60 km east of Toronto The overburden at the site varies between 21 to 36 m consisting of surficial lacustrine deposits and varved silt and clay which is underlain by dense to very dense sandy to silty tills. Beneath the overburden, the first 8 m of rock is a dark brown fossiliferous thin to medium bedded shaly limestone of Whitby Formation. The next 50 m of rock is limestone of the Lindsey Formation, which is mainly a fine-grained, fossiliferous, and massively bedded grey limestone. Testing on rock samples from the site showed that E_h = 46 GPa. The ratio between the horizontal to vertical modulus (E_h : E_v) varied from 1.1 to 1.5, with an average of 1.2. Therefore the rock was weakly anisotropic (Lo and Lukajic, 1984). Please refer to Figures 16 and 17 for detailed views of the Darlington site.

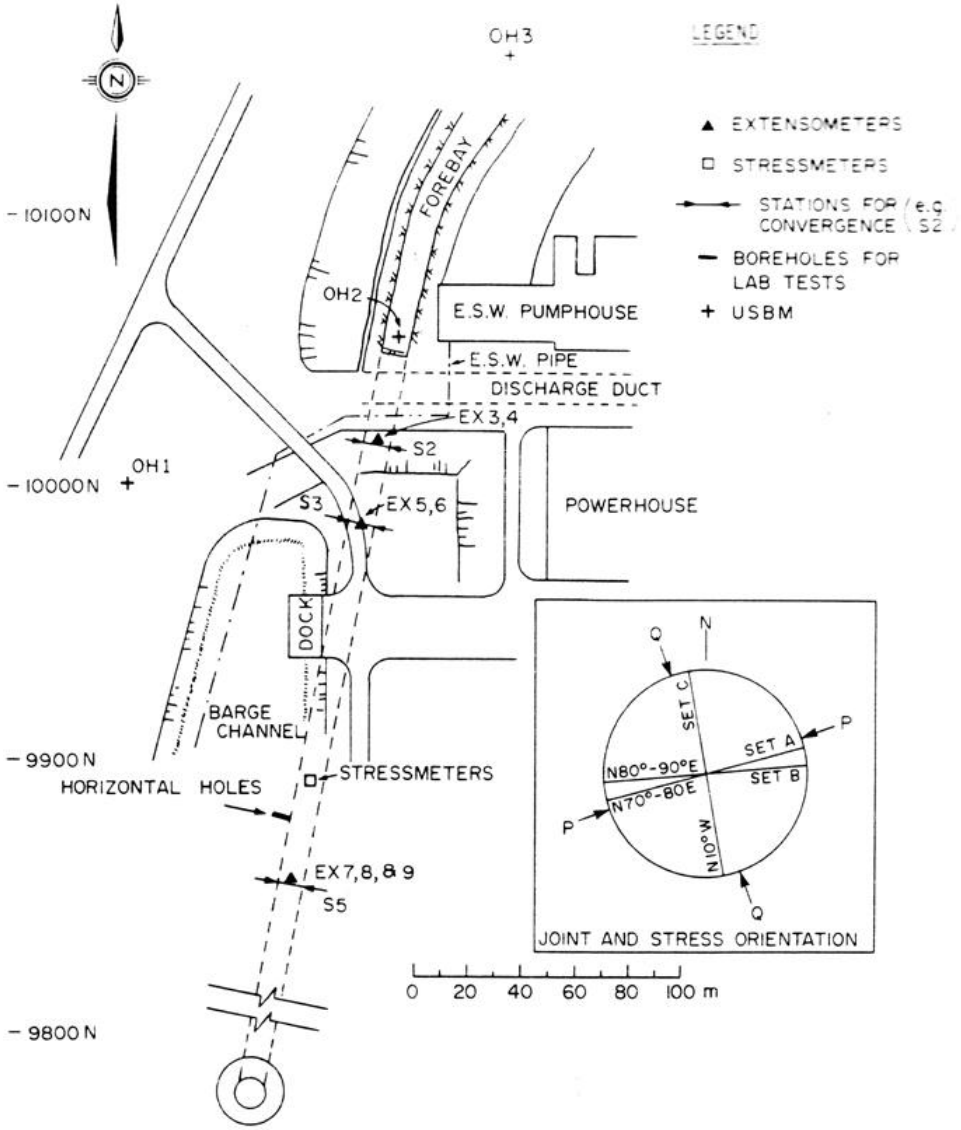

Figure 16. Plan View of the Darlington Tunnel (After Lo & Lukajic, 1984)

High horizontal stresses are common in the rock formations in Southern Ontario. These need to be evaluated and analysed before undertaking any tunnel design. Based on hydrofracturing methods, it was found that the state of horizontal stresses is very anisotropic. It was also found that based on the alignment and elevation of the tunnel the ratio of the horizontal to vertical initial stresses is approximately 10 at the springline (Lo and Lukajic, 1984). The base isotropic case of E = 30 MPa, ν = 0.33, γ = 25 kN/m^3, and K_0 = 10 was chosen because this closely matched the site conditions at the Darlington Tunnel. For the anisotropic case, E_h = 36 GPa, E_v = 30 GPa, ν = 0.33, K_0 = 10 and γ = 25 kN/m^3 were used. The field data were then used to validate the model for this case,

and a comparison is presented in Table 1 below. These site data were recovered from extensometers (A through F as seen in Figures 16 and 17) that were placed during the excavation process of the Darlington Tunnel. The constants generated by the regression procedure were then tabulated and were normalised relative to the Darlington example. As seen in Table 1, the numerical displacement values matched quite closely with the field values.

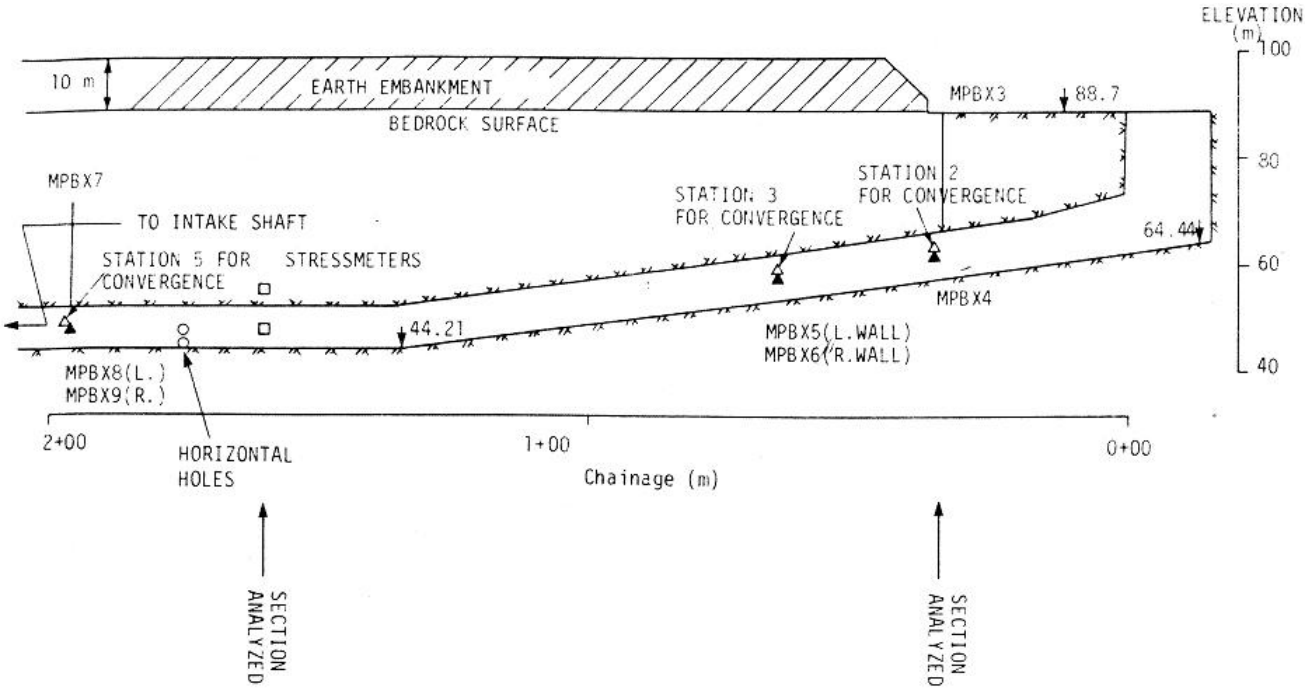

Figure 17. Elevation View of the Darlington Tunnel (After Lo & Lukajic, 1984)

Table 1. Comparison of Field Data with Numerical Data

Extensometer	Chainage	Absolute Displacement (mm)	Equivalent Chainage	Isotropic Displacement (mm)	Anisotropic Displacement (mm)
A	0+34.6	0.74	0+37.5	0.56	0.66
B		0.3		0.4	0.5
C		0.2		0.2	0.3
D	0+36	2.3	0+37.5	2.1	2.0
E		1.8		1.2	1.0
F		0.5		0.3	0.3

CONCLUSION

A preliminary description of the displacement profile near the advancing face of the tunnel under differing lateral stress conditions for both isotropic and anisotropic instances was presented. It was based on a deep tunnel opening in an elastic and isotropic medium. The parametric study that followed facilitated a simple tool for predicting the isotropic longitudinal displacement profile near the face as well as for the plane-strain regions. It was based on full, three-dimensional finite-element analyses. The results were checked against field measurements taken at the Darlington Tunnel of Southern Ontario. While an elastic solution is not realistic, it provides the engineer with a means for acquiring an excellent initial prediction of the longitudinal displacement profile in a tunnel as described above. Much work remains to be done to address this challenge posed by the variability in the observed displacement patterns around tunnels excavated in anisotropic media.

ACKNOWLEDGEMENT

We would like to express our gratitude to McGill University for providing us with the means for conducting our research, most specifically, the Department of Civil Engineering & Applied Mechanics.

REFERENCES

Carter, J.P., J.R. Booker (1990) Sudden Excavation of a Long Circular Tunnel in Elastic Ground. Int. J. Rock Mech. Min. Sci. & Geomech. 27, 129 – 132.

1. Corbetta, F., D. Bernaud, D. Nguyen-Mihn (1991) Contribution à la Méthode Convergence-Confinement par le Pricinpe de la Similitude. Rev. Franç. Géotech. 54, 5 – 11.

2. Eringen, A.C. (1957) Elasto-Dynamic Problem Concerning the Spherical Cavity. Q. J. Mech. Appl. Math. 10, 257 – 270.

3. Hefny, A.M., K.Y. Lo (1999) Analytical Solutions for Stresses and Displacements Around Tunnels Driven in Cross-Anistropic Rocks. International Journal for Numerical and Analytical Methods in Geomechanics. 23, 161 – 177.

4. Kumar, Prabhat (1986) Stress Concentration Due to Underground Excavation in Cross-Anisotropic and Nonhomogeneous Elastic Halfspace. Computers & Structures. 25, 687 – 694.

5. Lo, K.Y., B. Lukajic (1984) Predicted and Measured Stresses and Displacements Around the Darlington Intake Tunnel. Can. Geotech. J. 21, 147 – 165.

6. Morgan, H.D. (1961) A Contribution to the Analysis of Stress in a Circular Tunnel. Géotechnique. 11, 37 – 46.

7. Muir Wood, A.M. (1975) The Circular Tunnel in Elastic Ground. Géotechnique. 25, 115 – 127.

8. Panet, M., A. Guenot (1982) Analysis of Convergence Behind the Face of a Tunnel. In: Tunnelling ’82. The Institution of Mining and Metallurgy, London, 197 –204.

9. Pender, M.J. (1980) Elastic Solutions for a Deep Circular Tunnel. Géotechnique. 30, 216 – 222.

10. Selberg, H.L. (1952) Transient Compression Waves from Spherical and Cylindrical Cavities. Ark. Fys. 5, 97 – 108.

11. Sharan, S.K. (1989) Finite-Element Analysis of Underground Openings. Int. J. Num. & Ana. Meth. Geomech. 13, 565 – 570.

12. Sharpe, J. A. (1941) The Production of Elastic Waves by Explosion Pressures. Geophys. 7, 144 – 154.

13. Singh, B., R.K. Goel, V.K. Mehrotra, S.K. Garg, M.R. Allu,(1998) Effect of Intermediate Principal Stress on Strength of Anisotropic Rock Mass. Tunnelling and Underground Space Technology. 13, 71 – 79.

14. Singh, M., B. Singh, J.B. Choudhari, R.K. Goel (2004) Constitutive Equations for 3-D Anisotropy in Jointed Rocks and Its Effect on Tunnel Closure. Int. J. Rock Mech. Min. Sci. 41, 1 – 6.

15. Tonon, F., B. Amadei (2002) Effect of Elastic Anisotropy on Tunnel Wall Displacements Behind a Tunnel Face. Rock Mech. Rock Engng. 35, 141 – 160.

16. Verruijt, A. (1997) A Complex Variable Solution for a Deforming Circular Tunnel in an Elastic Half-Plane. International Journal for Numerical and Analytical Methods in Geomechanics. 21, 77 – 89.

17. Xiao, B., J.P. Carter (1993) Boundary Element Analysis of Anisotropic Rock Masses. Engineering Analysis with Boundary Elements. 11, 293 – 303.